

The *C. elegans* gene *pag-3* is homologous to the zinc finger proto-oncogene *gfi-1*

Yiwen Jia^{*,‡}, Guofeng Xie^{*,‡}, Joan B. McDermott and Eric Aamodt[†]

Louisiana State University Medical Center-Shreveport, P.O. Box 5932, Shreveport, Louisiana 71130-3932, USA

^{*}The first two authors contributed equally to this work

[†]Author for correspondence (e-mail: eaamodt@omvs.lsumc.edu)

[‡]Present address: Los Alamos National Laboratory, Cell and Molecular Biology Group, Mail Stop M888, Los Alamos, NM 87545, USA

SUMMARY

Mutations in the *Caenorhabditis elegans* gene *pag-3* result in misexpression of touch receptor-specific genes in the BDU interneurons and in motility defects. We cloned *pag-3* and found that the gene encodes a C₂H₂-type zinc finger protein related to the mammalian GFI-1 protein. Sequencing of the three *pag-3* alleles showed that two apparent null alleles encode a nonsense mutation before the zinc fingers and a missense mutation in the fourth zinc finger that changes a coordinating histidine to a tyrosine. The third allele contains a nonsense mutation in the N-terminal region but is not a null allele. Northern analysis showed that a single *pag-3* transcript of about 1.6 kb is present in embryos and L1, L2 and L3 larvae. *pag-3* message levels were about twofold higher in *pag-3* mutants than in wild-type animals, which suggested that *pag-3* may negatively regulate its own expression. *pag-3lacZ* fusion genes were expressed in the BDU interneurons, the touch neurons, 11 VA and 11 VB ventral cord motor neurons, two AVF interneurons and in unidentified neurons of the retrovesicular ganglion. The BDU neurons and the ALM touch neurons are lineal sister cells in the AB.a lineage and the VA and VB motor neurons are lineal sister cells in the AB.p

lineage. The VA motor neurons are required for backward movement and the VB motor neurons are required for forward movement. Mosaic analysis showed that the wild-type *pag-3* gene is required in the AB.p lineage for coordinated movement and in the AB.a lineage to suppress touch neuron gene expression in the BDU neurons. Because *pag-3* is expressed in both the BDU neurons and in the touch neurons, another protein(s) not expressed in the touch neurons may interact with *pag-3* to repress touch neuron gene expression in the BDU neurons. Alternatively, another protein in the touch receptor cells may inactivate PAG-3 and allow expression of the touch receptor program. These results show that *pag-3* is a temporally regulated gene that is expressed early in development and functions in multiple types of neurons. They also strongly suggest that the PAG-3 protein is a DNA-binding protein with properties similar to the mammalian proto-oncogene product GFI-1.

Key words: *Caenorhabditis elegans*, zinc finger, proto-oncogene, cellular differentiation, gene expression, touch receptors, motor neurons, tumorigenesis

INTRODUCTION

We are interested in how patterns of gene expression are established during development. The touch receptor neurons of the nematode *C. elegans* have been extensively characterized and provide a defined group of cells with which to address this problem (Chalfie, 1993; Chalfie and Au, 1989; Chalfie and Sulston, 1981; Chalfie and Thomson, 1982; Mitani et al., 1993; Xue et al., 1992, 1993). The genes that specify the touch cells apparently act in a combinatorial fashion, either to generate touch cells or to restrict their generation (Mitani et al., 1993). *unc-86* and *lin-32* encode transcription factors that are required to generate the touch neuron lineages (Chalfie, 1993). UNC-86 protein is thought to activate *mec-3*, which encodes a LIM-type homeodomain protein that is also required for the specification of the touch cell fate (Way and Chalfie, 1988, 1989). *mec-3* is expressed in ten cells: the six touch receptor neurons, the two FLP neurons and the two PVD neurons (Way and Chalfie,

1989). The MEC-3 and UNC-86 proteins are thought to form a heterodimer that activates genes required for touch cell function such as *mec-4* and *mec-7* (Chalfie, 1993). Negative regulation appears to be important for restricting the touch receptor fate to six cells: *lin-4* mutant animals misexpress *mec-4* and *mec-7* in the PVD neurons; *egl-44* and *egl-46* mutant animals misexpress *mec-4* and *mec-7* in the FLP neurons and *sem-4* mutant animals misexpress *mec-4* and *mec-7* in the PHC cells in the tail (Mitani et al., 1993; Basson and Horvitz, 1996). In addition, the cell-death genes *ced-3* and *ced-4* help to restrict the number of touch neurons, as mutations of those genes result in extra touch receptor cells (Mitani et al., 1993).

By staining *C. elegans* with fluorescent antibodies under conditions that do not kill embryos in gravid hermaphrodites (Jia et al., 1996; Xie et al., 1995), we screened for mutations that alter the expression of a *mec-7lacZ* fusion gene. *mec-7* encodes a β -tubulin that is highly expressed in the touch receptor neurons and is weakly expressed in the FLP, PVD and

BDU neurons (Hamelin et al., 1992; Mitani et al., 1993). We isolated several mutations that affected the PAttern of Gene expression (*pag*) of *mec-7lacZ* (Jia et al., 1996).

Mutations in *pag-3* result in misexpression of touch neuron genes in the BDU neurons (Jia et al., 1996). In addition to the *mec-7lacZ* reporter gene, the *mec-7*, *mec-2gfp*, *mec-4lacZ* and *mec-9lacZ* genes are also expressed in the BDU neurons of *pag-3* mutant animals. Mutations in *pag-3* do not appear to affect *mec-3lacZ* expression, but the expression of *mec-7* in the BDU neurons of *pag-3* mutants does require *mec-3(+)* (Jia et al., 1996). *pag-3* mutants also have motility defects: they are lethargic and show a reverse kinker uncoordinated (Unc) phenotype. This suggests that the PAG-3 protein is important for the development of other cells in addition to the BDU neurons and is involved in locomotion. Three *pag-3* alleles have been identified. All of the *pag-3* alleles are recessive to the wild-type allele and cause the Unc phenotype and misexpression of touch neuron genes in the BDU neurons. The *ls20* and *ls64* alleles cause similar phenotypes, whereas the *ls65* allele results in a slightly weaker Unc phenotype. *pag-3* was mapped to the right arm of the X-chromosome between *unc-3* and *unc-7*. Here we report the cloning and sequence analysis of *pag-3*, its pattern of expression and mosaic analysis of its function.

MATERIALS AND METHODS

Nematode strains and culture methods

C. elegans was cultured as described by Brenner (1974) and genetic nomenclature follows the guidelines of Hodgkin (1995). The wild-type strain was N2 var. Bristol. *pag-3* alleles *ls20*, *ls64* and *ls65* were described in Jia et al. (1996). Mutations used in this study were: *unc* (UNCoordinated), *pag* (PAttern of reporter Gene expression abnormal), *daf* (abnormal DAuer Formation), *osm* (defective avoidance of high OSMotic strength) and *sup* (SUPpressor). The alleles used were: *LGIII*, *unc-93(e1500)*; *LGX*, *unc-3(e151)*, *daf-6(e1377)*, *pag-3(ls20)*, *unc-7(e5)*, *osm-1(p808)*, *sup-10(mn219)* and *sup-10(n983)*. The free duplication *mnDp14* and the integrated *mec-2gfp* array *uls9* were used in the mosaic analysis. The extrachromosomal *pag-3lacZ* array *lsEx24* was used in analysis of *pag-3* expression in *pag-3* mutant animals.

Germ-line transformation rescue

Germ-line transformation was done by the procedure of Mello et al. (1991). To allow identification of the transgenic lines, plasmid pRF4 containing the semidominant *rol-6(su1006)* allele, which confers a roller phenotype, was co-injected at 80 ng/ μ l. The following YACs and cosmids were tested: Y70D2, Y37H4, R1178, C27C12, T28G8, T28D11, M03F9, C18B12, K11C2 and F09B12. YAC DNA was injected at about 5 ng/ μ l. Cosmid DNA was isolated by the alkaline lysis method (Sambrook et al., 1989) and was injected as single cosmids or in pairs at 15–30 ng/ μ l for each cosmid. Phage DNA was isolated by the plate lysate method for the rapid analysis of bacteriophage λ isolates (Sambrook et al., 1989). Phage DNA was injected alone or in pools of 5–10 phage at 5–10 ng/ μ l for each phage. Restriction fragments from the rescuing phage YJ1 were purified on gels and injected at 5 ng/ μ l.

Isolation of YAC DNA and construction of a phage library

We separated Y37H4 YAC DNA by pulse field gel electrophoresis (Chu et al., 1986; Schwartz and Cantor, 1984), with a 1% low melting point agarose gel in 0.5 \times TBE at 4°C (Sambrook et al., 1989). The gel slice containing the YAC DNA was digested with agarase, and the

DNA was either precipitated for microinjection or concentrated with a Centricon 10 microconcentrator (Amicon). We constructed a phage library in the λ GEM-11 vector (Promega) by the method of Whittaker et al. (1993). About 400 ng of YAC DNA was partially digested with *Mbo*I in the presence of *dam* methylase. The *Mbo*I sticky ends were partially filled in with dATP and dGTP, ligated into the phage vector, packaged and plated in strain LE392 following the manufacturer's protocols. We recovered 110 phage with an average insert size of about 20 kb.

Northern analyses

C. elegans (0.2–2.0 g) were grown on egg-yolk plates as previously described (McDermott et al., 1996), cleaned by sucrose flotation as described (Sulston and Hodgkin, 1988) and frozen in liquid nitrogen. Total RNA was isolated by the method of Maes and Messens (1992) with an additional chloroform extraction. The RNA samples (20 μ g) were treated with glyoxal-dimethyl sulfoxide, electrophoresed in 100 mM phosphate buffer (pH 6.5) and transferred to a MagnaCharge (MSI) nylon membrane (Ausubel et al., 1993). The blots were pre-hybridized for 2 hours and then hybridized overnight at 65°C in Church hybridization buffer (Church and Gilbert, 1984). The blots were washed twice in 2 \times SSPE, 0.1% SDS, then twice in 0.1 \times SSPE, 0.1% SDS at 50°C for 15 minutes each. Probes against *pag-3* RNA were made from a 1.0-kb *pag-3* cDNA fragment generated by PCR as described below; probes against *act-1* RNA were made from a 210 bp fragment from the 3' untranslated region of *act-1* isolated from the plasmid pT7-T3-18-1 (Krause et al., 1989). A Prime-It RmT Random Primer Labeling kit (Stratagene) was used. A Phosphor Imager screen and Image Quant software (Molecular Dynamics) were used to measure hybridization intensity.

Generation of *pag-3* cDNA fragments by PCR

We screened 1.5 \times 10⁶ plaques of a mixed stage *C. elegans* cDNA library (Stratagene), but did not recover any *pag-3* cDNA clones, so we generated overlapping *pag-3* cDNA fragments by the reverse transcription-polymerase chain reaction (RT-PCR) from wild-type and all three *pag-3* mutant strains. cDNAs were synthesized from 20 μ g total RNA with M-MuLV reverse transcriptase (New England Biolabs). The reactions were carried out at 37°C for 1 hour with 50 pmoles of an oligo(dT) primer [5'-GACTCGAGTTCGACATCGA(T)_{17-3'}]. The 5' cDNA fragments were amplified by PCR with the transcribed leader 1 (SL1) primer (5'-GGTTTAATTACCCAAGTTTGGAG-3') and L1, a primer specific to the zinc finger region (see below and Fig. 1). 3' cDNA fragments were generated by 3'RACE (Frohman et al., 1988) with the U1 and U3 primers and the oligo(dT) primer used in the reverse transcription reactions. Amplifications were performed with Taq DNA polymerase (Perkin-Elmer Cetus) under standard conditions. The PCR fragments were ligated into the pGEM-T vector (Promega).

DNA sequencing

A 5 kb *Xho*I-*Kpn*I genomic DNA fragment containing *pag-3* was ligated into pBluescript (Stratagene) to generate pYJ5 and was partially sequenced. Subclones containing unidirectional deletions for sequencing were generated with the Erase-a-Base kit (Promega) with exonuclease III. Sequencing was performed with the Sequenase 2.0 kit (US Biochemicals) and T7 and SP6 primers. Gaps in the sequence were filled in with the following oligonucleotide primers:

U1, 5'-TGTGAATACTGTGGAAAAGAT-3'
 U2, 5'-CTAACCTTATCACCCACAC-3'
 U3, 5'-GTGTTGAATCGTTACTCTCG-3'
 U4, 5'-CCGAGGAAATGGAGGAGTGA-3'
 U5, 5'-TGCGTGTCTGCTTCTCAAA-3'
 U6, 5'-GAGTGATGATGAAGAGGAG-3'
 U7, 5'-CTGAGGAGTATGGCAATTGG-3'
 L1, 5'-AAGGTTAGAAGACTGACTGA-3'
 L2, 5'-ATCAATTTACCAACATACCTG-3'

L3, 5'-TGAATCAGAAGGTGTGTAGA-3';
 L4, 5'-TCATACTCCTGAGGTATTGC-3';
 L5, 5'-CTTTCTCCTCTTCATCATC-3';
 L6, 5'-TAACATCGCAATACCATAAA-3';

Overlapping *pag-3* cDNA fragments were generated as described above. Both strands of the cDNA fragments were sequenced. For each mutant allele, a single RT-PCR-generated clone was sequenced, and another two independent PCR products were sequenced to confirm each mutation. Sequences were assembled with the DNAsis program (Hitachi Software Engineering). Sequence analyses were done with the Wisconsin package of programs (Genetics Computer Group, 1994). The sequence of the wild-type cDNA was deposited in GenBank (Accession # U63996).

Reporter plasmid transformation and staining

To construct a *pag-3lacZ* fusion gene, a partially digested 1.1-kb *XbaI* fragment from the plasmid pYJ5 spanning the first four exons and extending 400 bp upstream was cloned into the *C. elegans* expression vector pPD21.28 (Fire et al., 1990) to generate the plasmid pGX1. (The 5' *XbaI* site was from the pBluescript vector.) An overlapping 2.2 kb *XbaI* fragment from the phage YJ105 with a 3' endpoint just upstream of the first exon was inserted into pPD21.28 to produce pGX2. A 1.8 kb *PstI-XhoI* fragment from pGX2 was inserted into pGX1 to generate the plasmid pGX3. (The *PstI* site was from pPD21.28.) Thus, pGX3 contains approximately 2.2 kb of the *pag-3* promoter sequence, and 700 bp downstream encoding the amino-terminal 142 amino acids of the PAG-3 protein, which is fused to the *lacZ* coding region of pPD21.28 (see Fig. 4). The same sequences were introduced into the green fluorescent protein (*gfp*) expression vector TU#61 (Chalfie et al., 1994) to generate a *pag-3gfp* fusion gene.

Plasmid DNA was purified with the Wizard miniprep DNA purification system (Promega) and injected into the syncytial gonad of wild-type adult hermaphrodites as previously described (Mello et al., 1991). The *rol-6(su1006)*-containing plasmid pRF4 was co-injected as a marker for identifying transgenic animals. Each plasmid was injected at a concentration of 100 µg/ml. Transgenic animals were fixed and stained for β-galactosidase activity (Xie et al., 1995) with XAPI (4,6-diamidino-2-phenylindole) to visualize the positions of nuclei. Alternatively, fixed animals were stained with rat polyclonal anti-β-galactosidase antiserum and rhodamine-conjugated secondary antibody (Xie et al., 1995). *lacZ*-positive cells were identified on the basis of their positions relative to other nuclei and by their axonal morphologies. The relative positions and axonal morphologies of the BDU interneurons, the touch neurons, the VA and VB motor neurons and the AVF interneurons have been described (Sulston, 1976; Sulston and Horvitz, 1977; Sulston et al., 1983; White et al., 1986).

Mosaic analysis

Animals mosaic for *pag-3* were generated with duplication *mnDp14* and identified by the uptake of fluorescein isothiocyanate (FITC) in their phasmid and amphid neurons. The FITC staining protocol was described by Hedgecock et al. (1985). Strain EA185 (*unc-93; pag-3 unc-7 sup-10 osm-1; mnDp14*) was made from the following strains: EA92 (*pag-3; him-5*), SP1490 (*daf-6 unc-*

7 sup-10; mnDp14) and SP1528 (*unc-93; unc-3 unc-7 sup-10 osm-1; mnDp3*). Strain EA181 (*daf-6 pag-3*) was constructed from EA138 (*unc-3 pag-3*) and SP1490. Strain EA186 (*daf-6 pag-3 sup-10*) was constructed from strain EA181 and EA96 (*lin-15 sup-10*). Strain EA187 (*pag-3; mnDp14*) was constructed from EA92 and SP1490. Strain EA188 (*pag-3 sup-10 osm-1*) was constructed from strain SP1491 (*unc-7 sup-10 osm-1; mnDp3*) and EA128 (*pag-3 lin-15*). Strain EA189 (*daf-6 pag-3 sup-10; mnDp14*) was constructed from strain EA186, SP1490 and EA81 (*pag-3*). Strain EA197 (*pag-3 sup-10 osm-1; mnDp14*) was constructed from strain EA188, SP1490 and EA81. Strain EA208 (*pag-3 sup-10 osm-1; uls9; mnDp14*) was constructed from EA197 and TU2162 (*uls9*).

RESULTS

Cloning of *pag-3*

We cloned the *pag-3* gene by genetic mapping and germ line transformation rescue experiments as summarized in Fig. 1. *pag-3* was mapped between two previously cloned genes, *unc-3* and *unc-7*, on the right arm of the X-chromosome about 0.6

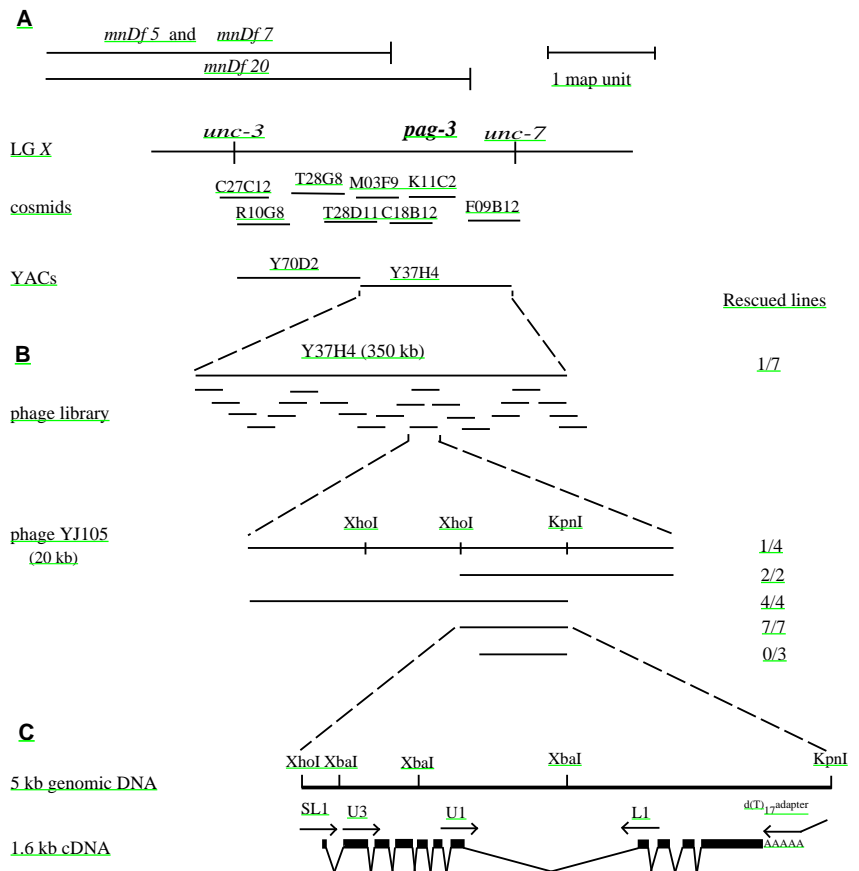


Fig. 1. *pag-3* cloning strategy and gene structure. (A) Genetic and physical maps of the *pag-3* locus showing the relative positions of the cosmids and YACs injected. Deficiencies used to map *pag-3* are indicated at the top. (B) Transformation rescue with YAC Y37H4-derived phage and fragments. (C) Restriction map of the 5-kb *XhoI*-*KpnI* fragment containing *pag-3*. The structure of the *pag-3* gene and 1.6-kb cDNA is shown below. The *pag-3* transcript begins with the trans-spliced leader SL1 at the 5' end, and ends with a poly(A) tail. The intron/exon boundaries were determined by comparing genomic and cDNA sequences. The trans-spliced SL1 exon and the ten exons of *pag-3* are represented as boxes. Oligonucleotide primers used to generate cDNA fragments are indicated by arrows.

map units to the right of *unc-3* (Jia et al., 1996). We transformed *pag-3*(*ls20*) animals with yeast artificial chromosomes (YACs) and cosmids in that interval and tested the transgenic lines for rescuing activity. The 350-kb YAC Y37H4 rescued the *pag-3* Unc phenotype; however, none of the cosmids in that region rescued *pag-3*. This suggests that *pag-3* lies between cosmids K11C2 and F09B12 in the only region not covered by cosmids. We made a phage library from the YAC DNA and transformed *pag-3*(*ls20*) animals, first with pools of phage DNA and then with DNA from single phage. Phage YJ105 rescued the Unc phenotype. Restriction fragments from YJ105 were tested for rescuing activity, and a 5-kb *XhoI-KpnI* fragment rescued both the Unc and the misexpression phenotypes in all transformed lines. A smaller fragment, which has a 1.0 kb deletion from the *XhoI* end, failed to rescue *pag-3* mutants. Southern analysis indicated that *pag-3* is a single-copy gene (data not shown).

pag-3 encodes a zinc finger protein

We sequenced portions of the genomic *XhoI-KpnI* fragment and found two regions homologous to the zinc fingers of the mammalian proto-oncogene product GFI-1. We used oligonucleotide primers to these regions to generate overlapping *pag-3* cDNA fragments by RT-PCR extending 3' to the poly(A) tail and 5' to the trans-spliced leader 1 (SL1) sequence found on many *C. elegans* mRNAs. Oligonucleotides to the SL1 sequence and to a zinc finger-encoding exon (L1) were used to generate a 5' fragment of the cDNA, and oligonucleotides U1 and U3 were used with the oligo(dT) adapter primer to generate 3' fragments for sequencing (Fig. 1C). The combined fragments correspond to a cDNA of 1609 bp (Fig. 1C). Comparison of the genomic DNA and cDNA sequences indicated that there are ten exons spanning 4 kb (Fig. 1C). Because the *pag-3* transcript is trans-spliced to SL1 at the 5' end, the transcriptional start site is unknown, but presumably lies within the 421 bp upstream of the mRNA 5' splice site in the rescuing *XhoI-KpnI* genomic fragment. A polyadenylation signal was found 15 bp upstream of the poly(A) tail of the cDNA fragments, and about 500 bp from the 3' end of the genomic fragment. Thus, the rescuing genomic fragment apparently contains the entire *pag-3* gene.

The *pag-3* cDNA encodes a protein with five C₂H₂-type zinc fingers (Fig. 2). A single open reading frame generates a predicted protein of 336 amino acids when read from the first AUG codon. As shown in Fig. 3, the 127 amino acids spanning the zinc fingers of the PAG-3 protein are 77% identical and 82% similar to zinc fingers 2-6 of the rat GFI-1 protein (Gilks et al.,

1993). The fingers match the consensus Y/FXCX₂CX₃Y/FX₈HX₃H, and the third and fourth linkers match the consensus TGEKYX for the Krüppel class of zinc

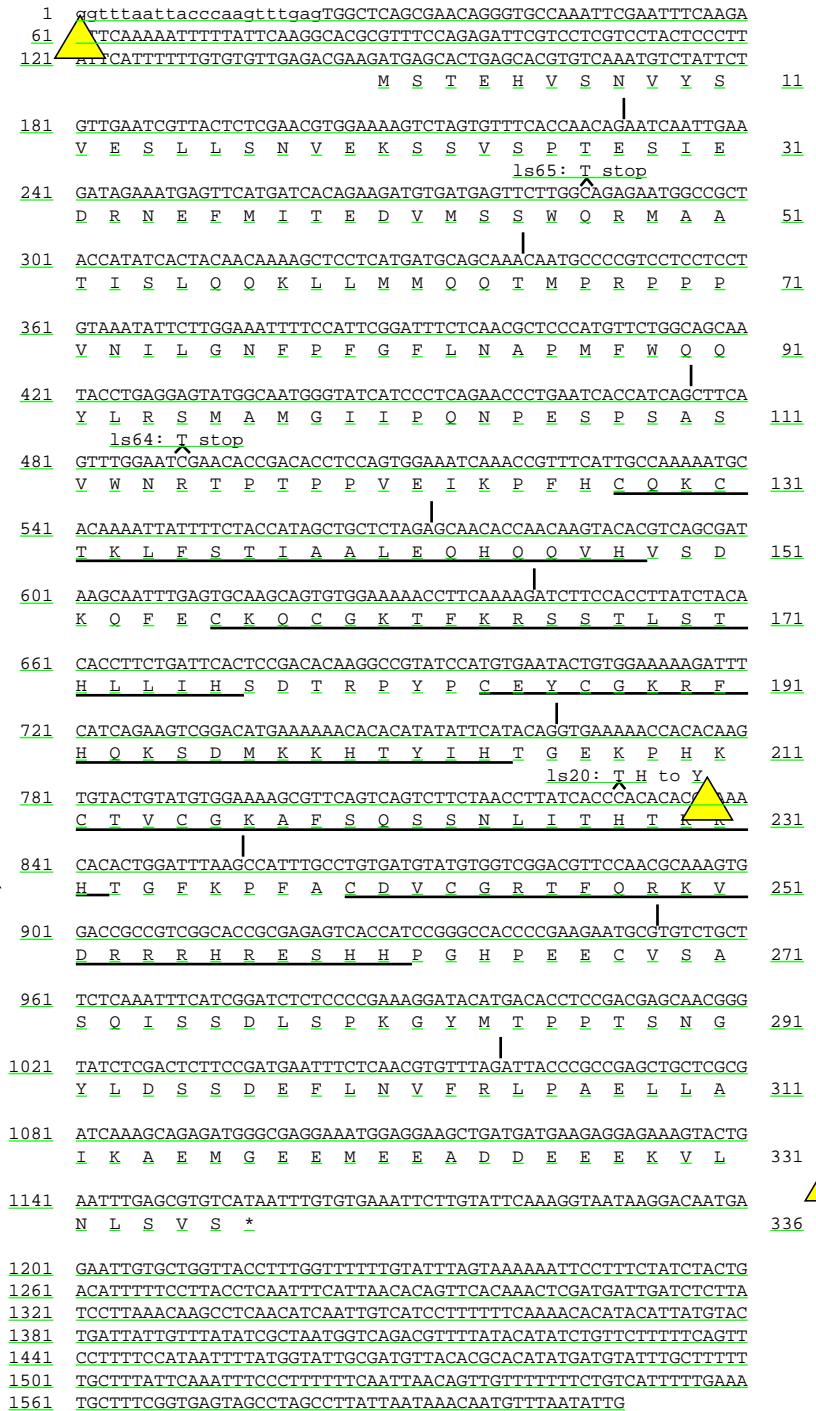


Fig. 2. *pag-3* cDNA and deduced amino acid sequences (GenBank Accession #U63996). The zinc fingers are underlined. The trans-spliced leader SL1 sequence is in lower case letters, the positions of introns are indicated with vertical lines, and the polyadenylation signal is double-underlined. The proline-rich region is between amino acids 67 and 125. The highly charged predicted α -helical region at the C terminus is between amino acids 304 and 331. For each mutant allele, the mutated base is marked by an arrowhead and the subsequent alteration in coding sequence is indicated. Nucleotide numbers are indicated on the left and amino acid numbers are indicated on the right. Amino acid numbering begins with the first AUG.

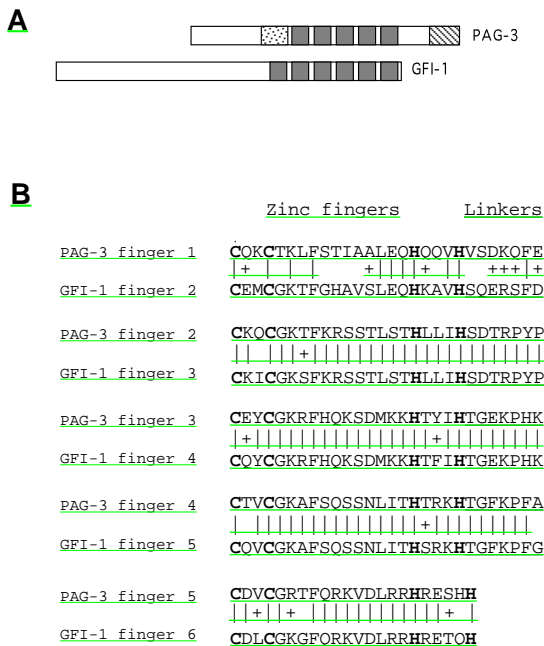


Fig. 3. Comparison of the structures of PAG-3 and GFI-1 and their zinc fingers. (A) The diagram represents the PAG-3 and GFI-1 proteins aligned at the region of homology. The gray boxes represent the five and six zinc fingers of PAG-3 and GFI-1, respectively. The proline-rich region of PAG-3 is indicated with a stippled box; the C-terminal predicted α -helical region is marked with a hatched box. (B) Alignment of the PAG-3 and GFI-1 zinc finger domains. Amino acid identities are indicated by ‘|’ and amino acid similarities by ‘+’. The sequences shown are continuous and correspond to amino acids 128 to 261 of the predicted PAG-3 protein, and 287 to 420 of the predicted GFI-1 protein. The residues predicted to form zinc fingers and linkers are indicated above the alignment. The coordinating cysteine and histidine residues are indicated with bold type and the linker regions are underlined. The third and fourth linkers of the PAG-3 protein match the consensus of the Krüppel class of zinc finger proteins.

finger proteins (Schuh et al., 1986). No other similarities were identified between PAG-3 and GFI-1 outside the zinc finger region. The GFI-1 open reading frame terminates after the zinc finger region, whereas the predicted PAG-3 protein extends an additional 76 amino acids beyond the fifth zinc finger (Fig. 3). Although no other defined motifs were identified in PAG-3, two other regions are worth noting. There is a proline-rich region from amino acid 61 to 125 (22% proline of 59 amino acids), and there is a region from amino acid 304 to 328 that is predicted to be α -helical and highly charged, especially over an acidic region (318-EEVTEADDEEE-328). The predicted α -helix would not be amphipathic.

Nature of the *pag-3* mutations

One point mutation was found in each of the *pag-3* mutant alleles (Fig. 2). cDNAs corresponding to each mutant allele were generated by RT-PCR. All mutations are C \rightarrow T transitions, a type of mutation often induced by EMS mutagenesis (Anderson, 1995). Previous studies have shown that the *pag-3*(*ls20*) and *pag-3*(*ls64*) alleles have the genetic characteristics of null alleles (Jia et al., 1996). The mutation in *pag-*

3(*ls20*) at nucleotide 829 changes a coordinating histidine in the fourth zinc finger (HIS 228) to a tyrosine. The mutation in *pag-3*(*ls64*) at nucleotide 490 introduces a stop codon 13 residues before the first zinc finger at ARG 115. Thus, the zinc finger domain, and the fourth zinc finger specifically, is essential for the function of PAG-3. The third allele, *pag-3*(*ls65*), is a hypomorph with the least severe effects on motility (Jia et al., 1996). The mutation in *pag-3*(*ls65*) introduces a stop codon (at GLN 47) upstream of several AUG codons, so translation of the mutant mRNA may initiate at a downstream AUG codon to generate a truncated protein with intact zinc fingers.

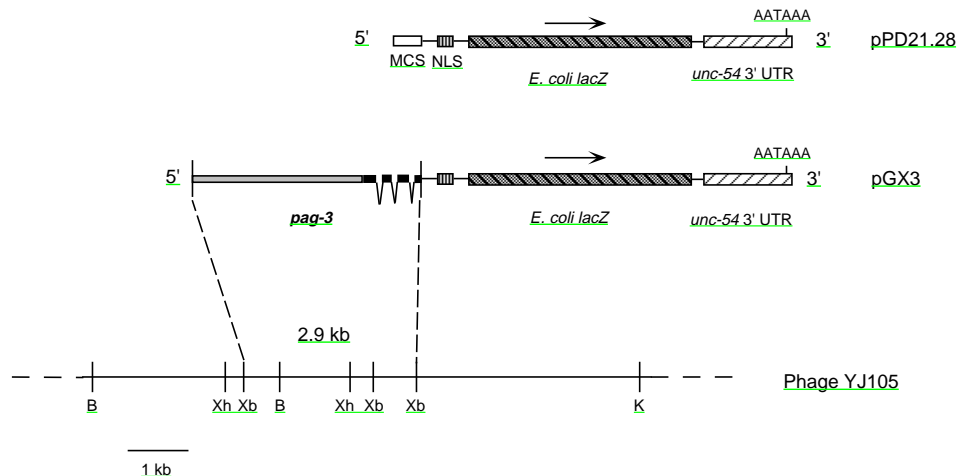
pag-3lacZ is expressed in the BDU neurons, the touch neurons, the VA and VB motor neurons, and two AVF interneurons

To determine where *pag-3* is expressed, we made a translational fusion construct with a 2.9-kb genomic fragment from the *pag-3* gene and the *E. coli lacZ* gene (Fig. 4). The 2.9-kb *pag-3* fragment includes about 2.2 kb of 5'-flanking sequence and encodes the N-terminal 142 amino acids. The vector includes a SV40 T-antigen nuclear localization signal. We transformed this fusion construct into wild-type *C. elegans* and obtained stable transgenic lines carrying the fusion gene in extrachromosomal arrays. We stained transgenic animals for β -galactosidase activity or with antibodies against β -galactosidase and examined them at all stages. The *pag-3lacZ* fusion gene was expressed in the BDU neurons and the six touch neurons (Fig. 5). Staining was also seen in 11 of 12 VA motor neurons, all 11 VB motor neurons, two AVF interneurons and the immediate precursors of all these cells (see Figs 5 and 6). Staining was seen not only in the nuclei, but also in the cell bodies and axons of the stained cells. The axonal trajectories of stained cells were clearly seen in transgenic animals stained with anti- β -galactosidase antibody. In addition, a few cells in the reticular ganglion were stained; one consistently stained well, others sporadically stained weakly. All the staining patterns observed with the *pag-3lacZ* construct were also observed with a *pag-3gfp* construct (data not shown).

The expression of *pag-3lacZ* in the BDU neurons and the ALM and PLM touch neurons was first seen in twofold stage embryos (data not shown) when *mec-7*, a touch neuron-specific gene, is first expressed. These neurons are generated in embryos at this stage (Sulston et al., 1983). The AVM and PVM touch neurons are derived post-embryonically at the L1 larval stage (Sulston and Horvitz, 1977), and were stained at this stage (Fig. 5A). Staining in all of these cells lasted until the early L2 stage.

Expression in the VA and VB motor neurons and their immediate precursors was observed in late L1 to early L2 stage transgenic animals (Fig. 5). The ventral nerve cord consists of eight distinctive classes of motor neurons (Sulston, 1976; Sulston and Horvitz, 1977; Sulston et al., 1983). Three classes (DA, DB and DD) are generated during embryogenesis. The remaining five classes (VA, VB, VC, AS and VD) are descendants of P neuroblasts and are postembryonically derived during late L1 and early L2 larval stages. The cell lineages that generate these five classes of motor neurons are depicted in Fig. 6. The positions of all the motor neurons in the ventral cord are relatively invariant, and they exhibit distinctive axonal

Fig. 4. *pag-3lacZ* reporter gene. The expression vector pPD21.28, the *pag-3lacZ*-containing plasmid pGX3 and the genomic region of *pag-3* in the phage YJ105 are shown. Arrows indicate the direction of transcription. The multiple cloning site (MCS), SV40 T-antigen nuclear localization signal (NLS) and *unc-54* 3'-untranslated region (UTR) with polyadenylation signal (AATAAA) are indicated in vector pPD21.28. The putative *pag-3* TATA box and position of the N-terminal exons (black boxes) are indicated in pGX3. The restriction sites in phage YJ105 are: B, *Bgl*III; K, *Kpn*I; Xb, *Xba*I; Xh, *Xho*I.



trajectories (White et al., 1986). Cells expressing *pag-3lacZ* have either anteriorly or posteriorly directed axons, which resemble the axonal morphologies of the V-type motor neurons (VA, VB and VC). The stained cells correspond in number and position to the VA and VB motor neurons. The remaining classes of motor neurons have not only anteriorly or posteriorly directed processes, but also commissures that run around to the dorsal cord. Staining was not observed in neurons with such commissures.

Northern analysis of total RNA from wild-type hermaphrodites at each developmental stage reflected the same pattern of temporal regulation (data not shown). A single transcript of about 1.6 kb is present in RNA from embryos and L1, L2 and L3 larvae and is most abundant in L2 larvae. The mRNA disappears in L4 larvae and young adults and reappears in mature adult hermaphrodites bearing embryos. Northern analysis of *pag-3* expression in wild-type and mutant animals showed that *pag-3* transcripts are produced at about twofold higher levels in mutant animals (data not shown).

Because the northern analysis suggested that *pag-3* negatively regulates its own expression, we examined the effect of *pag-3* mutations on the expression of the *pag-3lacZ* fusion gene. We introduced *pag-3* mutations into strains carrying the fusion gene. We did not detect any change of *pag-3lacZ* expression in embryos, L1 or L2 larvae. However, the ALM and PLM touch receptor neurons and the BDU neurons express the fusion gene at a higher frequency in L3, L4 and adult animals in *pag-3* mutant backgrounds than in the wild-type background (Table 1).

Mosaic analysis: what cells are responsible for the *pag-3* Unc phenotype?

To define the cell lineages that require *pag-3(+)* activity for coordinated locomotion, we used the method of Herman (1984, 1987, 1989) to generate mosaic animals. The locomotion of *C. elegans* is controlled by 75 motor neurons that innervate the ventral and dorsal body muscles (Chalfie and White, 1988), and coordination between the motor neurons is mediated by five pairs of interneurons. Motility defects could be due to muscle or neural defects. Almost all body wall muscle cells (94 of 95) descend from P₁, whereas 74 of 75 motor neurons are descendants of AB.p (Fig. 5).

The chromosomal location of *pag-3* enabled us to use a scheme very similar to that used for mosaic analysis of *unc-3* and *unc-7* (Herman, 1984, 1987; Starich et al., 1993). *pag-3* maps to the right arm of the X chromosome, in close proximity to *daf-6* and *osm-1* (Fig. 7A). Both genes are required for the uptake of FITC by the amphid neurons in the head and the phasmid neurons in the tail. *daf-6* or *osm-1* mutant animals carrying a chromosomal duplication of this region (*mnDp14*) were scored for FITC-staining pattern and motility phenotypes to determine at which cell division the duplication was lost.

To determine whether the Unc phenotype of *pag-3* mutants results from a muscle defect, we first identified mosaic animals that had lost the duplication in P₁. The strain we used has the genotype *unc-93(e1500) III; pag-3(ls20) unc-7(bx5) osm-1(p808) sup-10(mn219) X; mnDp14(X;f)[pag-3(+)] unc-7(+)* *osm-1(+)* *sup-10(+)*. *unc-93(e1500)* animals have the 'rubberband' phenotype: they contract and relax when they are prodded on the head (Greenwald and Horvitz, 1980). *sup-10(mn219)* is a recessive suppressor of *unc-93(e1500)* and has no phenotype alone (Greenwald and Horvitz, 1980). *unc-7(bx5)* animals exhibit a forward kinker Unc phenotype. *pag-3(ls20) unc-7(bx5)* double mutants show forward and reverse kinker Unc phenotypes. The dupli-

Table 1. Mutations in *pag-3* affect the expression of *pag-3lacZ* gene

Strain	Frequency (%) of detection* for each cell type in adult animals				
	ALM	BDU	PLM	AVM/PVM	Other†
Wild type (n=80)	2%	1%	7%	2%	3%
<i>pag-3(ls20)</i> (n=65)	38%	46%	35%	9%	69%
<i>pag-3(ls64)</i> (n=41)	60%	51%	58%	2%	90%
<i>pag-3(ls65)</i> (n=94)	11%	41%	22%	2%	95%

* 'Frequency of detection' refers to the occurrence of staining for a given cell type among all the animals.

† 'Other' refers to one unidentified cell stained in the retrovesicular ganglion.

Table 2. Phenotypes of *pag-3* mosaic animals

FITC-staining pattern	Point of Dp loss	Dp present in germ line	Number of mosaics
A. Strain genotype: <i>daf-6(e1377) pag-3(ls20) sup-10(n983); mnDp14</i> (Number of Dp-bearing animals screened: 25,900)			
No amphid or phasmid staining	AB or AB.p	±	18
No amphid or phasmid staining	AB or AB.p	=	4
Only right amphid and right phasmid stained	AB.pl	±	2
Only left amphid and left phasmid stained	AB.pr	±	2
B. Strain genotype: <i>pag-3(ls20) sup-10(n983) osm-1(p808); mnDp14</i> (Number of Dp-bearing animals screened: 15,700)			
No amphid or phasmid staining	AB	±	8
Only 4 left amphid cells stained*	AB.p	±	6
Only 4 left amphid cells, 5 right amphid cells and 1 right phasmid cell stained†	AB.pl+AB.pra	±	1
Only 1 left amphid cell and 1 left phasmid stained‡	AB.a+AB.pr+ AB.pla	±	2

*The staining amphid neurons are ADFL, ADLL, ASJL and ASKL.
 †The staining neurons are: left amphid, ADFL, ADLL, ASJL and ASKL; right amphid, ADFR, ADLR, ASIR, ASJR and ASKR; right phasmid, PHBR.
 ‡The staining neurons are left amphid ASIL and left phasmid PHBL.

tion *mnDp14* contains the dominant wild-type copy of *pag-3*, *unc-7*, *osm-1* and *sup-10*. When the duplication is lost, *sup-10(+)* is absent and the rubberband phenotype is suppressed. Thus, duplication-bearing animals have the rubberband phenotype while non-duplication-bearing animals have the forward and reverse kinker Unc phenotypes. Because the germ line descends from P₁, mosaic animals that have lost the duplication at P₁ produce only progeny without the duplication. Because the mutation *osm-1(p808)* acts cell-autonomously to prevent the uptake of FITC in 16 neurons that descend from AB.a and AB.p, the presence of the duplication in the AB lineage will render the animals FITC-staining. Thus, mosaics that have lost the duplication at P₁ [P₁(-)] are non-Unc-7, FITC-staining and non-rubberband, and they should have only forward and reverse kinker Unc, non-rubberband, FITC-nonstaining self-progeny. We screened for such animals and found 15 P₁(-) mosaics satisfying all of the above criteria from about 6200 duplication-bearing animals. All of these mosaics were wild type in locomotion. This result suggested that the wild-type *pag-3* gene product is not required in muscle cells for coordinated movement.

We then addressed whether *pag-3(+)* is required in cells derived from AB to promote coordinated movement. We used two strains to generate AB(-) mosaics. The first strain has the genotype: *daf-6(e1377) pag-3(ls20) sup-10(n983); mnDp14*. *sup-10(n983)* is another recessive allele of *sup-10*, which confers the rubberband phenotype described above for *unc-93* (Greenwald and Horvitz, 1986). *daf-6* acts cell-non-autonomously in the four sensory cells,

AMshL/R and PHshL/R, to assist FITC uptake by the amphid and phasmid neurons, respectively. Duplication-bearing self-progeny are wild type for movement and FITC-staining. Self-progeny without the duplication have the rubberband phenotype and are FITC-nonstaining due to the *daf-6* mutation. We first screened for *pag-3* reverse kinker Unc animals from the above strain and then analyzed their FITC-staining pattern to determine the point of duplication loss in the AB lineage. From about 25,900 duplication-bearing animals, 26 reverse kinker Unc mosaic animals were found. 22 of those segregated two types of progeny: FITC-staining animals of wild-type motility and rubberband, FITC-nonstaining animals. The inheritance of the staining phenotype

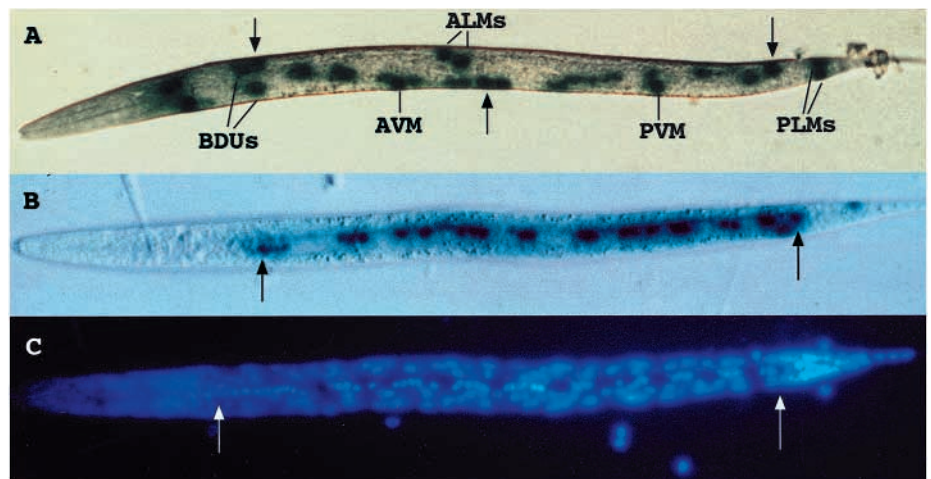
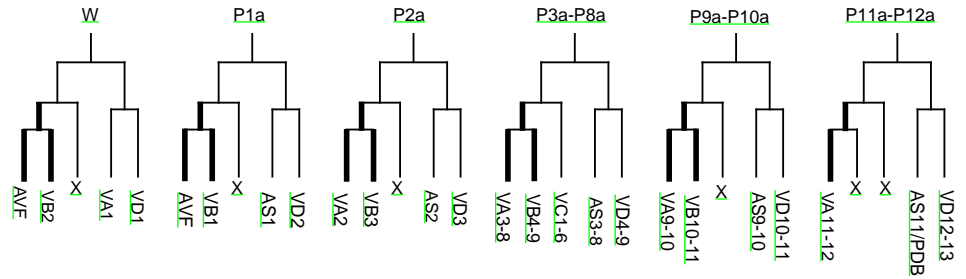


Fig. 5. *pag-3lacZ* expression. *pag-3lacZ* is expressed in the touch neurons (ALMs, AVM, PVM and PLMs), the BDU neurons, 11 VA and 11 VB motor neurons, 2 AVF interneurons and some neurons in the retrovesicular ganglion. (A) Lateral view of a late L1 transgenic animal bearing the *pag-3lacZ* array *lsEx24* stained for β -galactosidase. The ventral cord containing the VA and VB motor neurons twists around the animal due to the *rol-6* marker gene used to follow transformation. (B and C) Ventral view of a late L1 transgenic animal stained for β -galactosidase activity (B) and with DAPI for the visualization of nuclei (C). The *lacZ*-positive cells between the arrows in A and B are the VA and VB motor neurons in the ventral cord. The arrows in B and C mark the same positions of the ventral nerve cord. Staining for β -galactosidase obscures the DAPI signal. Anterior is to the left.

Fig. 6. Simplified postembryonic cell lineages of the motor neurons. The thickened lines indicate the neurons expressing *pag-3lacZ*. The 11 VA and 11 VB motor neurons, 2 AVF interneurons and their immediate precursors, which expressed *pag-3lacZ*, are derived from 13 neuroblasts (W and P1a-P12a). VA1, the VA motor neuron which does not express *pag-3lacZ*, is derived from the posterior daughter of the W neuroblast. X, cell death.



showed that *mnDp14* had been maintained in the mosaic parent's germ line that is derived from P_a. The remaining four *pag-3* mosaics had only rubberband offspring, which indicated that the mosaic parents had lost *mnDp14* in the germ line. The points of duplication loss of the *pag-3* mosaics are summarized in Table 2A.

The second strain that we used to screen for AB(-) mosaics has the genotype: *pag-3(ls20) sup-10(n983) m-1(p808); mnDp14*. Self-progeny with the duplication are wild type and FITC-staining. Self-progeny without the duplication have the rubberband phenotype and are FITC-nonstaining. Of about 15,700 duplication-bearing animals screened, 17 reverse kinker Unc mosaic animals were found (Table 2B).

Because all 43 *pag-3* reverse kinker Unc mosaics obtained from both strains showed duplication losses at AB or AB.p, the focus of *pag-3* action is probably distributed among descendants of AB.p. During the course of mosaic analysis, we noted that many mosaic animals had experienced more than one duplication loss. We also found a number of *pag-3* reverse kinker Unc mosaic candidates that were later shown by progeny testing to not be true mosaics. Most of these individuals seemed to contain partially deleted duplications. Both phenomena have been observed in several other mosaic analysis experiments (Greenwald and Horvitz, 1986; Herman, 1984, 1987; Starich et al., 1993; Villeneuve and Meyer, 1990).

What cells are required for the *pag-3* expression phenotype?

To identify the cells that are responsible for the misexpression phenotype conferred by mutations in *pag-3*, we constructed a strain of genotype *pag-3(ls20) sup-10(n983) osm-1(p808); uls9; mnDp14*. The integrated *mec-2gfp* array *uls9* was used as a marker for scoring the misexpression phenotype. 14 *pag-3* reverse kinker Unc mosaics were found from about 19,500 duplication-bearing animals. These mosaics were examined for *mec-2gfp* expression in their BDU neurons and then for their points of duplication loss by FITC uptake (Table 3). Because duplication loss in AB was sufficient to cause the misexpression phenotype while duplication loss in AB.p did not lead

to the misexpression phenotype, the focus of *pag-3* action is very likely among descendants of AB.a, from which the ALM and BDU neurons are derived.

DISCUSSION

The *C. elegans pag-3* gene represses touch neuron-specific genes in the BDU neurons and is required for coordinated movement (Jia et al., 1996). We have cloned and sequenced *pag-3* and investigated where *pag-3(+)* is required and when and where *pag-3(+)* is expressed. *pag-3* encodes a C₂H₂-type zinc finger protein with zinc fingers that are highly homolo-

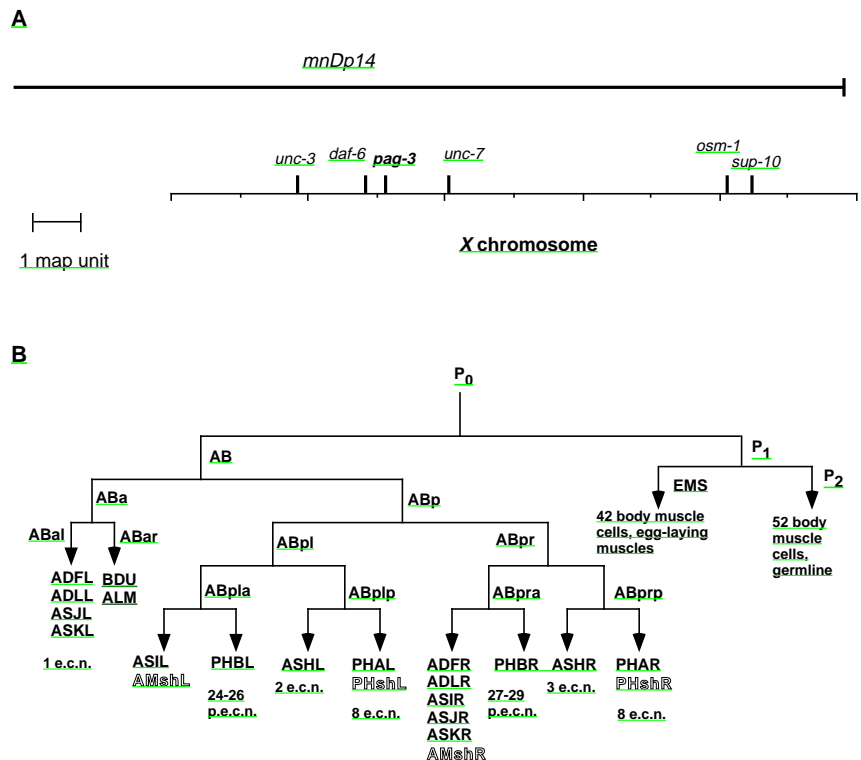


Fig. 7. (A) Genetic map of *pag-3* on the X chromosome and the free duplication *mnDp14*. The positions of each of the genes used for the mosaic analysis of *pag-3* are shown. *mnDp14* contains wild-type copies of all the genes indicated. (B) *C. elegans* cell lineage showing the early cell divisions and the cells affected by the mutations that were used in the genetic mosaic analysis. P₀ is the zygote. L and l represent left, and R and r represent right. AB.al, AB.pl and AB.pr generate amphid and phasid neurons (capital letters) and sheath cells (outlined letters). The origins of embryonically derived cord motor neurons (e.c.n.) and postembryonically derived cord motor neurons (p.e.c.n.) are also indicated. The BDU and ALM cells derive from the AB.ar lineage and are underlined.

Table 3. Phenotypes of *pag-3* mosaic animals

FITC-staining pattern	Point of Dp loss	BDU <i>mec-2gfp</i> fluorescence	Dp present in germ line?	Number of mosaics
No amphid or phasmid staining	AB	±	±	14
Only 4 left amphid cells stained*	AB.p	—	±	1
All 6 left amphid cells and all left phasmid cells stained	AB.pr	—	±	2

Strain genotype: *pag-3(ls20).sup-10(n983).osm-1(p808);uls9:mnDp14*.
 Number of Dp bearing animals screened: 19,500.
 *The staining amphid neurons are ADfL, ADLl, ASJL and ASKL.

gous to those encoded by a mammalian proto-oncogene, *gfi-1*. Expression analyses showed that *pag-3* transcription is regulated during development and that *pag-3* negatively regulates its own expression. A *pag-3lacZ* fusion gene was expressed in the BDU neurons, the touch neurons, VA and VB motor neurons, the AVF neurons and unidentified neurons of the retrovesicular ganglion. Mosaic analysis showed that *pag-3* functions in the AB.a lineage to promote the fate of the BDU neurons, and in the AB.p lineage to promote locomotion. Together these results show that *pag-3* is expressed in and is required in multiple types of neurons.

Because PAG-3 is a zinc finger protein, it probably binds DNA and acts as a transcriptional regulator. At least four genes expressed in touch neurons (*mec-2gfp*, *mec-4lacZ*, *mec-7* and *mec-9lacZ*) are negatively regulated by *pag-3* in the BDU neurons (Jia et al., 1996; G. Xie and E. Aamodt, unpublished results), and *pag-3* also negatively regulates its own expression. The allele *ls64*, which encodes a truncated protein without the zinc finger region, and the *ls20* allele, which has a missense mutation at a zinc-binding histidine in the fourth zinc finger, have the genetic characteristics of null alleles. This suggests that the zinc finger region is essential for the function of PAG-3. The N-terminal proline-rich region of PAG-3 may function in transcriptional regulation (Ma and Ptashne, 1987; Mitchell and Tjian, 1989).

The sequence similarity of the zinc fingers encoded by *pag-3* and *gfi-1* is striking and suggests conservation of function. The amino acid sequences are 77% identical between zinc fingers 1-5 in PAG-3 and zinc fingers 2-6 in GFI-1, and 89% identical between the last four zinc fingers in these two proteins. The sequence similarity of these zinc fingers suggest that they may bind to a similar DNA sequence, but DNA binding seems insufficient to explain this level of sequence conservation. That is, certain residues of C₂H₂ zinc fingers have been shown through crystallography to contact DNA (Pavletich and Pabo, 1991, 1993; Pieler and Bellefroid, 1994) or to be important for DNA site selection (Pavletich and Pabo, 1991), but other residues face away from the DNA helix and do not seem to be critical for binding. Because the region of sequence conservation between these two proteins is continuous in the zinc finger domain, we postulate that the whole region is important to the functions of these proteins, and that they will have not only similar binding sites, but other functional similarities. For example, both PAG-3 and GFI-1 may interact with other proteins through their zinc finger domains. *gfi-1* (Growth Factor Independence-1), was identified from a viral insertion that rendered interleukin-2 (IL-2)-dependent T-cell lymphoma lines IL-2-independent (Gilks et al., 1993). Zornig et al. (1996) found that *gfi-1* cooperates with two other oncogenes, *myc* and *pim-*

1, in lymphomagenesis. GFI-1, like PAG-3, may be a transcriptional repressor (Zweidler-McKay et al., 1996).

Expression of *pag-3* coincides with the generation of touch and motor neurons, and may be negatively self-regulated. A *pag-3lacZ* fusion gene was expressed in the touch neurons and BDU neurons from the time of their generation to the L2 larval stage, and in the VA and VB motor neurons and the AVF interneurons from late L1 to L2 larval stages (Fig. 5). This expression pattern is consistent with the results from the developmental northern analysis (not shown), which showed that *pag-3* mRNA was present from the embryonic to the L3 stage and peaked during the L1 and L2 stages. Northern analysis showed higher *pag-3* mRNA message levels in mixed-stage populations of *pag-3* mutants than in wild type (not shown), and we found that the *pag-3lacZ* transgene was expressed into adulthood more frequently in *pag-3* mutant animals (Table 1). These results suggest that *pag-3* may negatively regulate its own expression late in development. Although Pulak and Anderson have shown that the presence of in-frame stop codons decreases the stability of a message, particularly near the 5' end (Pulak and Anderson, 1993), we observed a twofold increase in message levels of the *pag-3(ls65)* mRNA, which encodes a stop in the predicted N-terminal region. Thus, either the stop codon did not destabilize the *pag-3(ls65)* message or the loss of autoregulation of *pag-3* more than compensated for this destabilization.

Genetic mosaic analysis suggested that *pag-3(+)* is required in the AB.a lineage to prevent the misexpression phenotype and in the motor neurons of the AB.p lineage to promote locomotion. The BDU neurons and the ALM touch neurons are descendants of AB.a. Mosaic animals that have lost the duplication at AB ectopically express *mec-2gfp* in the BDU neurons, whereas AB.p(−) mosaics do not. We can conclude from this study that the activity of the gene is required in the AB.a lineage, but we are unable to determine more precisely in what sublineage *pag-3* acts.

Loss of *pag-3(+)* in the progenitors of the motor neurons rather than in the progenitors of the body muscle cells led to motility defects. The cord motor neurons descend from AB, and 74 of 75 of the cells are descendants of AB.p. Half of the VA and VB motor neurons descend from AB.pl, and the rest descend from AB.pr. All but one body muscle cell descend from P₁. All P₁(−) mosaics were wild type in locomotion and all *pag-3* reverse kill mosaic animals had the duplication loss in the AB or AB.p lineages. Because the loss of duplication at either AB.pl or AB.pr resulted in *pag-3* Unc animals, *pag-3(+)* is required in both of these lineages. We did not find any *pag-3* Unc mosaic animals that had lost the duplication solely in the AB.a lineage, so it is unlikely that *pag-3(+)* is required in AB.a to coordinate movement.

The VA motor neurons are required for backward movement whereas the VB motor neurons are required for forward locomotion. *pag-3* mutant animals exhibit both backward and forward locomotion defects (Jia et al., 1996). Wild-type *C. elegans* move forward and backward with a smooth sinusoidal movement, but *pag-3* mutant animals are lethargic and are unable to propagate a smooth sinusoidal movement when moving backwards. Instead, they make irregular bends. This phenotype is referred to as a reverse kinker uncoordinated phenotype. The forward movement of *pag-3* mutants is also affected, in that they move forward slowly when prodded. These defects probably result from the loss of *pag-3(+)* activity in either the VA or VB motor neurons or in both.

In an earlier report, we postulated that PAG-3 helps to differentiate the ALM and BDU neurons by repressing the touch neuron genes in the BDU neurons (Jia et al., 1996). The data reported here on the *pag-3* sequence and mosaic analysis supported this model, but we were surprised to find that *pag-3lacZ* is expressed in the BDU neurons and in the touch neurons at comparable levels. Why does *pag-3* prevent touch neuron gene expression in the BDU neurons but not in the touch neurons? Clearly another factor must differentiate the ALM and BDU neurons. One strong candidate for such a factor is MEC-3. MEC-3 and UNC-86 are thought to act together to activate the touch neuron genes (Lichtsteiner and Tjian, 1995; Xue et al., 1993). *unc-86* is expressed in both the BDU neurons and in the touch neurons, but *mec-3* is apparently only expressed at observable levels in the touch neurons and in four other cells: the PVD neurons and the FLP neurons (Way and Chalfie, 1989). *mec-3lacZ* expression is not detected in the BDU neurons (Way and Chalfie, 1989); however, we found that expression of *mec-7lacZ* in the BDU neurons of *pag-3* mutant animals requires *mec-3* (Jia et al., 1996). Perhaps, then, *mec-3* is expressed at a high level in the touch neurons but at a very low level in the BDU neurons, and PAG-3 and MEC-3 act competitively by binding to the same or overlapping sites. MEC-3 predominates in the touch neurons to activate touch neuron genes, and PAG-3 represses touch neuron genes in the BDU neurons where MEC-3 levels are low. We tested this prediction with *pag-3(ls20)* and two hypomorphic *mec-3* alleles, *u298* and *u312* (data not shown). In both cases, the presence of a mutated *pag-3* gene did not affect the frequency at which *mec-7lacZ* was expressed in the touch neurons. These experiments assume that the *pag-3(ls20)* product has lost DNA-binding activity and that the MEC-3 protein in these strains can bind its targets. The nature of the *mec-3* lesions is not known, however, so this experiment does not entirely rule out the possibility of a PAG-3:MEC-3 competition.

The role of *pag-3*, if any, in determination of cellular fate in asymmetric cell divisions remains to be elucidated. The ALM touch neurons and the BDU interneurons are lineal sister cells (Sulston et al., 1983) that have distinct morphologies and perform different functions: the two ALM cells are touch receptor neurons, while the two BDU neurons are interneurons of unknown function (Chalfie and Au, 1989; Chalfie and Sulston, 1981; White et al., 1986). Likewise, the VA and VB motor neurons are sister cells that have distinct morphologies and functions (Chalfie and White, 1988; White et al., 1986). The AVF interneurons derive from the W and P1a neuroblasts in lineages parallel to those of the VA motor neurons. As a putative DNA-binding protein, PAG-3 may contribute to fate

determination as a transcriptional repressor since loss-of-function mutations in *pag-3* caused ectopic expression of touch neuron genes in the BDU neurons, and since PAG-3 represses its own expression in the ALM and BDU neurons late in development (Table 1). PAG-3 may directly bind its own control regions and those of several touch neuron genes to prevent transcription of these genes. Alternatively, *pag-3* may affect the transcription of touch neuron genes indirectly by activating downstream activators and repressors. In either case, PAG-3 must act together with another protein(s) not expressed in the touch neurons to repress touch neuron gene expression in the BDU neurons, or another protein in the touch receptor cells may inactivate PAG-3 and allow expression of the touch receptor program. The identification of potential binding sites for PAG-3 in genes expressed either in the touch neuron or the motor neuron lineages may clarify the mechanism of PAG-3 activity.

We thank M. Chalfie for the *mec-2gfp* array *uls9*; J. Shaw for strains SP1490, SP1491 and SP1528; M. Krause for plasmid pT7-T3-18-103, R. Holmgren for the anti- β -galactosidase antiserum, and A. Coulson for cosmids and YACs. We are grateful to X. Alvarez-Hernandez and J. Glass for the use of their microscope, D. Gross for the CHEF gel apparatus, P. Good and L. Robinson for supplies and discussions, S. Aamodt for the staged RNAs and for helpful discussions and comments on this manuscript, T. Harrington and K. Simpson for technical assistance, and B. Norman for oligonucleotides. Some nematode strains were provided by the *Caenorhabditis* Genetics Center, which is funded by the National Institutes of Health National Center for Research Resources (NCRR). This study was supported by grants to E.A. from the LSU Medical Center-Shreveport, the Biomedical Research Foundation of Northwest Louisiana and the LSUMC Center for Excellence in Cancer Research.

REFERENCES

- Anderson, P. (1995). Mutagenesis. In *Caenorhabditis elegans: Modern Biological Analysis*, vol. 48 (ed. H. Epstein and D. Shakes), pp. 31-58. Academic Press, San Diego.
- Ausubel, F. M., Brent, R., Kingston, R. E., Moore, D. D., Seidman, J. G., Smith, J. A. and Struhl, K. (1995). *Current Protocols in Molecular Biology*. Current Protocols, New York.
- Basson, M. and Horvitz, H. R. (1995). The *Caenorhabditis elegans* gene *sem-4* controls neuronal and mesodermal cell development and encodes a zinc finger protein. *Genes Dev.* **10**, 1953-1965.
- Brenner, S. (1974). The genetics of *Caenorhabditis elegans*. *Genetics* **77**, 71-94.
- Chalfie, M. (1993). Touch receptor development and function in *Caenorhabditis elegans*. *J. Neurobiol.* **24**, 1433-1441.
- Chalfie, M. and Au, M. (1989). Genetic control of differentiation of the *Caenorhabditis elegans* touch receptor neurons. *Science* **243**, 1027-1033.
- Chalfie, M. and Sulston, J. (1981). Developmental genes of the mechanosensory neurons of *Caenorhabditis elegans*. *Dev. Biol.* **82**, 358-370.
- Chalfie, M. and Thomson, J. N. (1982). Structural and functional diversity in the neuronal microtubules of *Caenorhabditis elegans*. *J. Cell Biol.* **95**, 15-23.
- Chalfie, M., Tu, Y., Euskirchen, G., Ward, W. Y. and Prasher, D. C. (1994). Green fluorescent protein as a marker for gene expression. *Science* **263**, 802-804.
- Chalfie, M. and White, J. (1988). The nervous system. In *The nematode Caenorhabditis elegans* (ed. W. B. Wood), pp. 337-392. Cold Spring Harbor Laboratory.
- Chu, G., Vollrath, D. and Davis, K. W. (1986). Separation of large DNA molecules by contour-clamped homogenous electric fields. *Science* **234**, 1582-1585.
- Church, G. M. and Gilbert, W. (1984). Genomic sequencing. *Proc. Nat. Acad. Sci. USA* **81**, 1991-1995.
- Fire, A., Harris, S. W. and Dixon, D. (1990). A modular set of *lacZ* fusion

- vectors for studying gene expression in *Caenorhabditis elegans*. *Gene* **93**, 189-198.
- Frohman, M. A., Dush, M. K. and Martin, G. R. (1988). Rapid production of full-length cDNAs from rare transcripts: amplification using a single gene-specific oligonucleotide primer. *Proc. Nat. Acad. Sci. USA* **85**, 8998-9001.
- Genetics Computer Group (1994). *Program Manual for the Wisconsin Package, Version 8*. Genetics Computer Group, 575 Science Drive, Madison, Wisconsin, USA 53711.
- Gilks, C. B., Bear, S. E., Grzes, L. and Tschlis, P. N. (1993). Progression of interleukin-2 (IL-2)-dependent rat T cell lymphoma lines to IL-2-independent growth following activation of a gene (*Gfi-1*) encoding a novel zinc finger protein. *Mol. Cell. Biol.* **13**, 1759-1768.
- Greenwald, I. S. and Horvitz, H. R. (1980). *unc-1500*: a behavioral mutant of *Caenorhabditis elegans* that defines a gene with a wild-type null phenotype. *Genetics* **96**, 147-164.
- Greenwald, I. S. and Horvitz, H. R. (1986). A visible allele of the muscle gene *sup-10 X* of *Caenorhabditis elegans*. *Genetics* **113**, 63-72.
- Hamelin, M., Scott, J. M., Wang, C. and Culotti, J. G. (1991). The *mec-7* β -tubulin gene of *Caenorhabditis elegans* is expressed primarily in the touch receptor neurons. *EMBO J.* **11**, 2885-2893.
- Hedgecock, E. M., Culotti, J. G., Thomson, J. and Perkins, L. A. (1985). Axonal guidance mutants of *Caenorhabditis elegans* identified by filling sensory neurons with fluorescent dyes. *Dev. Biol.* **111**, 158-170.
- Herman, R. K. (1984). Analysis of genetic mosaics of the nematode *Caenorhabditis elegans*. *Genetics* **108**, 165-180.
- Herman, R. K. (1991). Mosaic analysis of genes that affect nervous system structure in *Caenorhabditis elegans*. *Genetics* **116**, 377-388.
- Herman, R. K. (1989). Mosaic analysis in the nematode *Caenorhabditis elegans*. *J. Neurogenetics* **5**, 1-44.
- Hodgkin, J. (1995). *Caenorhabditis elegans*. *Trends Genet. Genetic Nomenclature Guide*, 24-25.
- Jia, Y., Xie, G. and Aamodt, E. (1996). *pag-3*, a *C. elegans* gene involved in touch neuron gene expression and coordinated movement. *Genetics* **142**, 141-147.
- Krause, M., Wild, M., Rosenzweig, B. and Hirsh, D. (1989). Wild-type and mutant *unc-49* genes. *Caenorhabditis elegans*. *J. Mol. Biol.* **208**, 381-392.
- Lichtsteiner, S. and Tjian, R. (1995). Synergistic activation of transcription by UNC-86 and MEC-3 in *Caenorhabditis elegans* embryo extracts. *EMBO J.* **14**, 3937-3945.
- Ma, J. and Ptashnik, M. (1987). A new class of yeast transcriptional activators. *Cell* **51**, 113-119.
- Maes, M. and Meselson, E. (1992). Phenol as grinding material in RNA preparations. *Nucl. Acids Res.* **20**, 4374.
- McDermott, J. B., Aamodt, S. and Aamodt, E. (1996). *ptl-1*, a *Caenorhabditis elegans* gene whose products are homologous to the tau microtubule-associated protein. *Biochemistry* **35**, 9415-9423.
- Mello, C. C., Kramer, J. M., Stinchcomb, D. and Ambros, V. (1991). Efficient gene transfer in *C. elegans*: extrachromosomal maintenance and integration of transforming sequences. *EMBO J* **10**, 3959-3970.
- Mitani, S., Du, H., Hall, D. H., Driscoll, M. and Chalfie, M. (1993). Combinatorial control of touch receptor neuron expression in *Caenorhabditis elegans*. *Development* **119**, 773-783.
- Mitchell, P. and Tjian, R. (1989). Transcriptional regulation in mammalian cells by sequence-specific DNA binding proteins. *Science* **245**, 371-378.
- Pavletich, N. P. and Pabo, C. O. (1991). Zinc finger-DNA recognition: crystal structure of a Zif268-DNA complex at 2.1 Å. *Science* **252**, 809-817.
- Pavletich, N. P. and Pabo, C. O. (1993). Crystal structure of a zinc-finger-DNA complex: New perspectives on zinc fingers. *Science* **261**, 1701-1707.
- Pieler, T. and Bellefroid, E. (1994). Perspectives on zinc finger protein function and evolution-an update. *Mol. Biol. Rep.* **20**, 1-8.
- Pulak, R. and Anderson, P. (1993). mRNA surveillance by the *Caenorhabditis elegans smg* genes. *Genes Dev.* **7**, 1885-1897.
- Sambrook, J., Fritsch, E. F. and Maniatis, T. (1989). *Molecular Cloning: A Laboratory Manual, Second Edition*. Cold Spring Harbor Laboratory Press, Cold Spring Harbor, New York.
- Schuh, R., Aicher, W., Gaul, U., Grotz, S., Preiss, A., Maier, D., Selfert, E., Nauber, U., Schreiner, C., Krieger, R. and Jackle, H. (1986). A conserved family of zinc finger proteins containing structural elements of the finger protein encoded by *Krüppel*, a *Drosophila* segmentation gene. *Cell* **47**, 1025-1032.
- Schwartz, D. C. and Cantor, C. R. (1984). Separation of yeast chromosomesized DNAs by pulsed field gradient gel electrophoresis. *Cell* **37**, 67-75.
- Starich, T. A., Herman, R. K. and Shaw, J. E. (1993). Molecular genetic analysis of *unc-7*, a *Caenorhabditis elegans* gene required for coordinated locomotion. *Genetics* **133**, 527-541.
- Sulston, J. and Hodgkin, J. (1991). Methods. In *The Nematode Caenorhabditis elegans* (ed. W. B. Wood). Cold Spring Harbor Laboratory Press, Cold Spring Harbor, New York.
- Sulston, J. E. (1976). Post-embryonic development in the ventral cord of *Caenorhabditis elegans*. *Philos. Trans. R. Soc. Lond. B* **275**, 287-298.
- Sulston, J. E. and Horvitz, H. R. (1977). Post-embryonic cell lineages in the nematode *Caenorhabditis elegans*. *Dev. Biol.* **56**, 110-156.
- Sulston, J. E., Schierenberg, J., White, J. G. and Thomson, J. N. (1983). The embryonic cell lineage of the nematode *Caenorhabditis elegans*. *Dev. Biol.* **100**, 64-119.
- Villeneuve, J. M. and Meyer, B. J. (1990). The role of *sdc-1* in the sex determination and dosage compensation decisions in *Caenorhabditis elegans*. *Genetics* **124**, 91-114.
- Way, J. C. and Chalfie, M. (1988). *mec-3*, a homeobox-containing gene that specifies differentiation of the touch receptor neurons in *C. elegans*. *Cell* **54**, 5-16.
- Way, J. C. and Chalfie, M. (1989). The *mec-3* gene of *Caenorhabditis elegans* requires its own product for maintained expression and is expressed in three neuronal cell types. *Genes Dev.* **3**, 1823-1833.
- White, J. G., Southgate, E., Thomson, J. N. and Brenner, S. (1986). The structure of the nervous system of *Caenorhabditis elegans*. *Philos. Trans. R. Soc. Lond. B* **314**, 1-340.
- Whittaker, P. A., Moulton, M. and Wood, L. (1993). Construction of phage sublibraries from nanogram quantities of YAC DNA purified by preparative PFGE. *Trends Genet.* **9**, 195-196.
- Xie, G., Jia, Y. and Aamodt, E. (1995). *C. elegans* mutant screen based on antibody or histochemical staining. *Genetic Analysis Techniques and Applications* **12**, 95-100.
- Xue, D., Finney, M., Ruvkun, G. and Chalfie, M. (1992). Regulation of the *mec-3* gene by the *C. elegans* homeoproteins UNC-86 and MEC-3. *EMBO J.* **11**, 4969-4979.
- Xue, D., Jia, Y. and Chalfie, M. (1993). Cooperative interactions between the *Caenorhabditis elegans* homeoproteins UNC-86 and MEC-3. *Science* **261**, 1324-1328.
- Zornig, M., Staudt, T., Karsunky, H., Grzeschiczek, A. and Moroy, T. (1996). Zinc finger protein *GFI-1* cooperates with *MYC* and *PIM-1* in T-cell lymphomagenesis by reducing the requirements for IL-2. *Oncogene* **12**, 1789-1801.
- Zweidler-Mckay, P. A., Grimes, H. L., Flubacher, M. M. and Tschlis, P. N. (1996). *Gfi-1* encodes a nuclear zinc finger protein that binds DNA and functions as a transcriptional repressor. *Mol. Cell. Biol.* **16**, 4024-4034.